

MLS based Distributed, Bearing, Range and Posture Estimation for Schools of Submersibles

Navinda Kottege & Uwe R. Zimmer

Research School of Information Sciences and Engineering
Autonomous Underwater Robotics Research Group
The Australian National University, ACT 0200, Australia ¹

navinda.kottege@anu.edu.au | uwe.zimmer@ieee.org

Continuous relative localization among all local members of a school of submarines is an essential pre-condition for distributed motion control. Exploiting the short-range, underwater electromagnetic as well as the acoustical channel, the proposed approach delivers sufficient bearing, range and posture estimations based on local sensing in small, autonomous submersibles with limited energy capacities and computational resources. This research is part of the Serafina project at the Australian National University, aiming for large schools of autonomous underwater vehicles.

Results of a number of physical experiments are presented which tests for precision, sensing range, interference robustness, and motion sensitivity.

1. Motivation

In order for underwater vehicles to behave as a swarm each member needs to know the positions and orientations of at least its near neighbours. The Serafina project ([1], [2], [10]) aims to have many small submersibles (about 50 cm in length) in large schools. While the small size imposes constraints in terms of size and energy consumption of the components the swarming behavior requires a high degree of flexibility as the spatial configuration changes frequently and fast.

The research is motivated by the need for a small, low-cost underwater localization and posture estimation system for the Serafina submersibles. The initial experiments presented in [7] showed that it is feasible to use an acoustic based system in order to achieve this objective. In this paper we further refine the techniques used and present results of more real world experiments conducted in the outdoor testing pool and in the Lake Burley Griffin².

¹. Parts of this project are supported by Advanced Technology Systems Australia (atsa), Newcastle, NSW, Australia



figure 1: Serafina MkII

2. Technical approach

Bearing Estimation

The method introduced in [7] uses wide-band acoustic signals which are transmitted from small Serafina submersibles and received on multiple miniature hydrophones on each neighbouring submersible enabling estimation of bearing and posture as seen from those neighbouring Serafinas. The relative bearing of the sending submersible can be calculated by measuring the phase shift of the received signal channels. The phase shift δ is obtained by cross-correlating the received signal channels (figure 7) and detecting the peak in the correlation curve. The relative bearing estimate θ_e of the sound source is given by:

$$\theta_e = \pm \text{atan} \left(\frac{\sqrt{d^2 - \delta^2}}{\delta} \right) \quad (1)$$

². Lake Burley Griffin is a lake with an approximate surface area of 6.64 km² situated in the centre of Canberra.

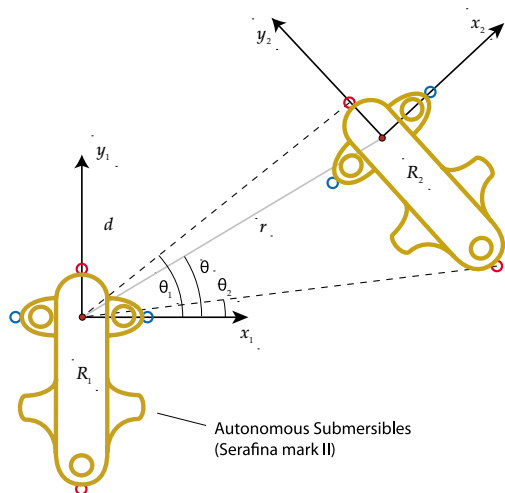


figure 2: Bearing and range definition

where d denotes the distance between receivers. The \pm sign in (1) denotes the front/back ambiguity arising in a two (omnidirectional) receiver setup. This problem is overcome by using multiple receiver pairs, or as in the presented experiments, employing directional hydrophones.

Range Estimation

The information received from the long wave and optical communication modules of the Serafina [3] is fused with the acoustic measurements to calculate the range information. The pulses of the acoustic localization system are synchronised to the omnicastr schedule introduced in [3] and simultaneously transmitted with the long wave radio packets. On the receiving vehicles, the arrival time of the electromagnetic signal t_e and the acoustic signal t_a gives the difference in the arrival times as t_r :

$$t_r = t_a - t_e \quad (2)$$

Considering the acoustical propagation speed v_a and electromagnetic propagation speed v_e underwater, the distance to the sending vehicle r can be calculated as follows:

$$r = \frac{t_r v_e v_a}{v_e - v_a} \quad (3)$$

Posture Estimation

Consecutively sending acoustic pulses from the projectors at the bow and aft ends of the submersible and separately cross-correlating the received signal pairs to obtain the relevant phase differences provides two bearing estimates for the two ends of the vehicle. Combining the range information with this gives the posture/orientation of the sending submersible. The main bearing measurement can be derived from the two end bearing measurements using

a weighted average depending on the actual positioning of the receivers on the submersible.

MLS Signals

In an underwater environment, acoustic signals are subject to many undesirable phenomena such as noise, fading, reflections, reverberations and multi-path propagation [8][9]. However in the setup under consideration, some problems faced by conventional underwater acoustic communication does not have an effect due to the very short ranges and low power used for transmission. After experimenting with a number of different types of acoustic signals, the most desirable characteristics were exhibited by Maximum Length Sequence (MLS) signals.

MLS signals have a quasi-flat frequency spectrum up to the Nyquist frequency. These signals can be classified as a type of white noise but are deterministic. Therefore it can be reproduced accurately. The most attractive feature of this type of signals is that they have a single sharp peak at zero in the auto-correlation graph. The theoretical characteristics of maximum length sequences (MLS) are well known and explored since the early 60's [4]. Using different generating polynomials will result in MLS signals of different length and there also can be different MLS signals of the same length. MLS Signals of arbitrary degree can be generated using a computer program developed by us. The degree n of the MLS signal governs the length l of the sequence as $l = 2^{n+1} - 1$.

The length of the sequence and the employed sampling rate of the digital to analog converter determines the duration of the outgoing signal. Even though longer MLS signals give better resolution of the cross-correlation peak resulting in higher precision of the estimated bearing, the longer duration has its drawbacks. They are: undesirable echoes in cluttered or enclosed environments, higher processing overhead, smaller frequency of estimates (f_E).

MLS signals of degree 6 (length 127) are employed as a compromise which gives a choice of 18 different signal forms of which some show a specifically small maximal cross-correlation.

System Overview

Figure 3 shows the main components of the bearing, range and posture estimation system. Even though each submersible would be equipped with both the sending and receiving system, for any given send-receive event, the sender and the receiver would be two different vehicles. The lower block represents the sender while the upper block represents the receiver. The longwave radio communication module is represented as one block and is not discussed in detail in this paper.

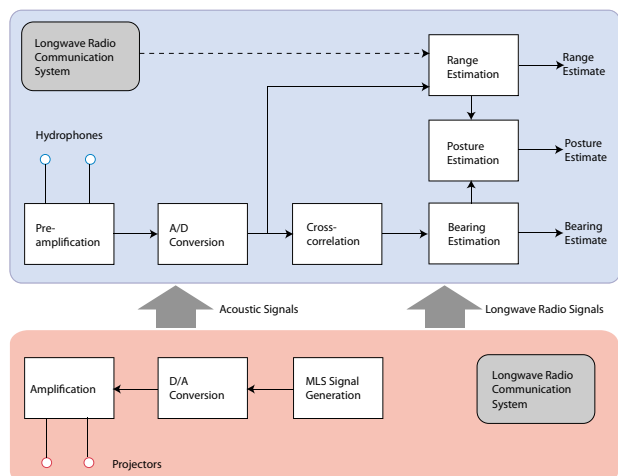


figure 3: The main components of the bearing, range and posture estimation system.

3. Experiments & results

Experimental Setup

Our current experimental setup employs four Benthos AQ2000 hydrophones, two as receivers and another two as the projectors. Two Serafina mock hulls with acoustic transducers are mounted on a gantry with two arms as shown in figure 4. The gantry is either placed on top of the outdoor testing pool (diameter: 4.2m, depth: 1.5m, medium: freshwater) immersing the hulls 1m underwater or connected to the end of a pier on the Lake Burley Griffin. This setup restricts the motion to one plane and therefore one pair of receiving hydrophones separated by a distance $d = 0.3\text{m}$ is sufficient.

The Serafina mock hull with the receiving hydrophones is connected to the gantry arm with a shaft that is mounted on a geared DC electric motor which

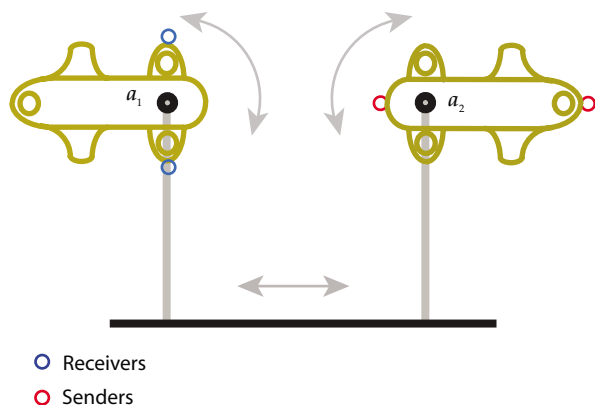


figure 4: Experimental setup

can rotate at constant low velocities (0.5 - 1.0rpm). Varying the supply voltage of the motor varies the angular velocity ω . The Serafina hull with the sending hydrophones can also be connected to the gantry arm with a shaft that can be arbitrarily oriented on the plane to suit the experiment. The distance r between the sending and receiving apparatus can be adjusted. The maximum separation for the experiments conducted so far have been limited by the physical size of the testing pool and the width of the pier on the lake. The mock hulls used in this setup is shown in figure 5.

An acoustic pulse train is sent out repeatedly from the projectors while the receiving hydrophones are being rotated around its shaft axis a_1 . The pulse train consists of length 127 MLS signals and 20kHz marker signals (figure 6). The signals arriving at the hydrophones are captured and recorded for off-line analysis. The frequency of the marker signal is selected to be the resonance frequency of the hydrophones. This provides distinct markers for slicing the long recorded signal into many small signal segments containing one MLS pulse per channel. These signal segments are used as inputs for the cross-correlation using the algorithm given in [6].

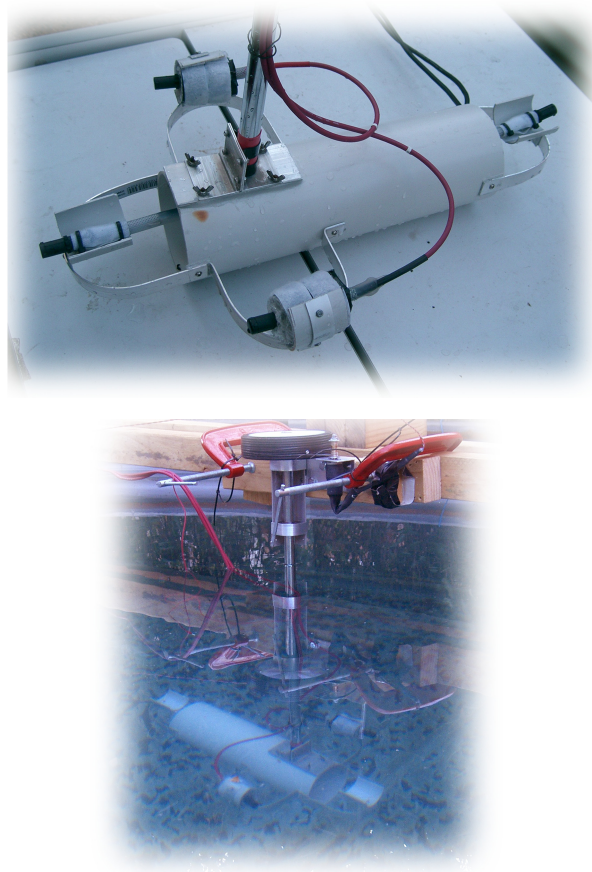


figure 5: Serafina mock hulls with the acoustic transducers

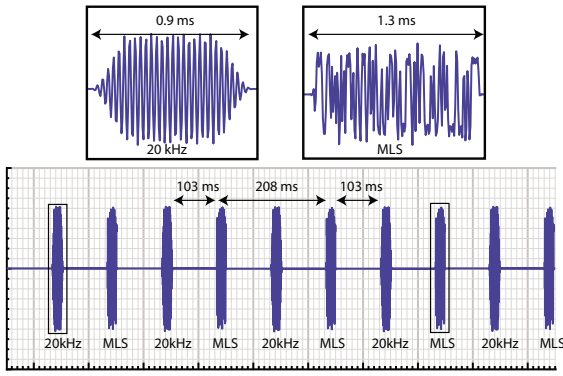


figure 6: Employed outgoing pulse train structure

The digital-to-analog conversion for the outgoing signals and analog-to-digital conversion for the incoming signals are implemented on a synchronized 24-bit 96kHz sampling device connected to a notebook computer. This sampling frequency gives a MLS signal duration of approximately 1.3ms and a gap of about 102ms between the MLS pulses and the marker signals is employed to ensure that all the reverberations off the pool walls have sufficient time to decay. Two consecutive MLS pulses have a gap of around 208ms which translates to a maximum estimate sampling rate of $f_E = 4.8\text{ Hz}$.

As the receiving hull is rotated ($\theta: 0^\circ \rightarrow 180^\circ$) the induced phase shift δ at the receiving hydrophone pair is given by:

$$\delta = \sqrt{(r \sin \theta)^2 + \left(r \cos \theta + \frac{d}{2}\right)^2} - \sqrt{(r \sin \theta)^2 + \left(r \cos \theta - \frac{d}{2}\right)^2} \quad (4)$$

where d is the distance between the receiving hydrophones and r is the distance between the sender and the receiver.

The phase shift (in sample points) between the channels is obtained by searching for the peak in the cross-correlation plot (figure 7). A cubic spline interpolation is used to interpolate peaks which lie in between sample points. By using an interpolation step of 0.1 samples the minimum achievable resolution is improved to 0.35° (for static measurements). In general the minimum achievable angular resolution (in the dynamical case – moving submersibles) R_{min} is given by:

$$R_{min} = \frac{\omega}{f_E} \quad (5)$$

Where ω is the angular velocity of the rotating receiver and f_E the estimate sampling rate.

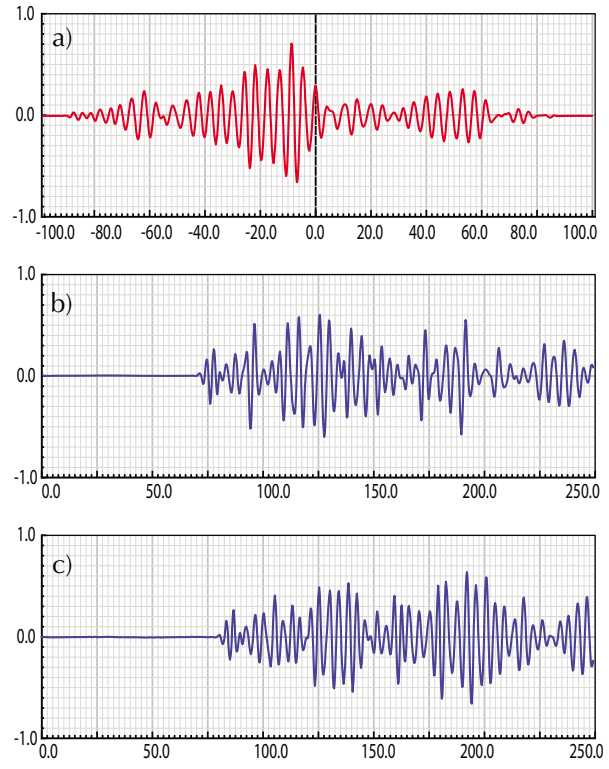


figure 7: b) and c) represent the received MLS signals normalized amplitudes over the samples; a) shows the MLS cross-correlation result over the sample-shift, corresponding to bearing $\theta = 120^\circ$ (actual bearing estimation $\theta_e = 119.8^\circ$ in this measurement; and in general $|\theta - \theta_e| < 8^\circ$).

The position on the x -axis (in sample points) which corresponds to the peak in the correlation plot is related to the actual phase shift δ (in metres) by:

$$\delta = \frac{x v_a}{f_s} \quad (6)$$

where f_s is the sampling frequency (96kHz in the current experiments) and v_a is the speed of sound in water (1475.5 ms^{-1} as calculated by Mackenzie's [5] nine-term equation with parameters $T = 18^\circ\text{C}$, $D = 1.0\text{ m}$ and $S = 0.073\text{‰}$).

Experimental Results

Many experiments with different r values and different angular velocities were conducted both in the test pool and the lake. Each cross-correlation of the two channels in a MLS signal segment constitutes a measurement and yields one bearing estimate. Each experiment consists of a series of such measurements obtained while the receiving hull is rotated at a uniform angular velocity producing a series of such bearing estimates. The presented graphs plot the calculated bearing estimate against the series of measurements.

Figure 8 and 9 shows plots of two experimental runs

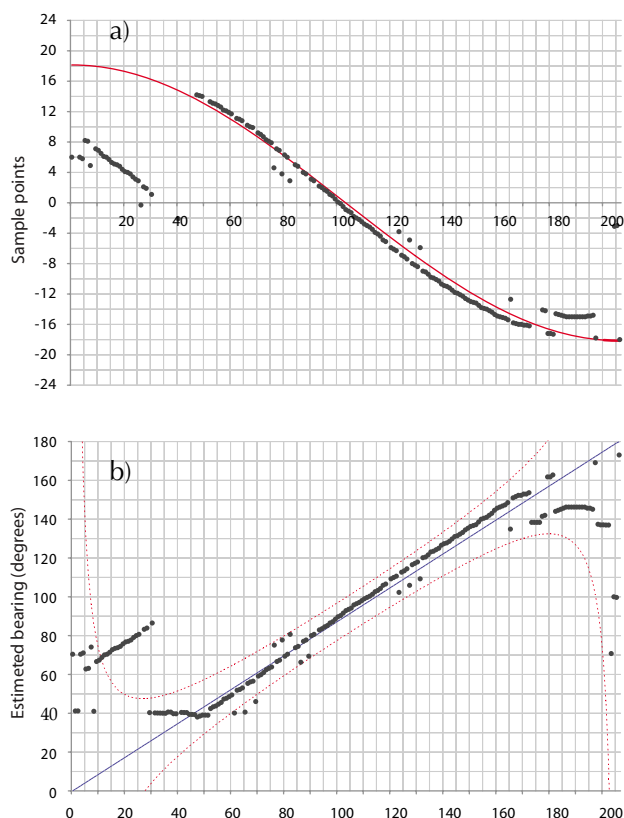


figure 8: $r = 0.8\text{m}$, Clockwise rotation; a) measured phase shift x over the series of measurements; b) estimated bearings with error margin over the series of measurements

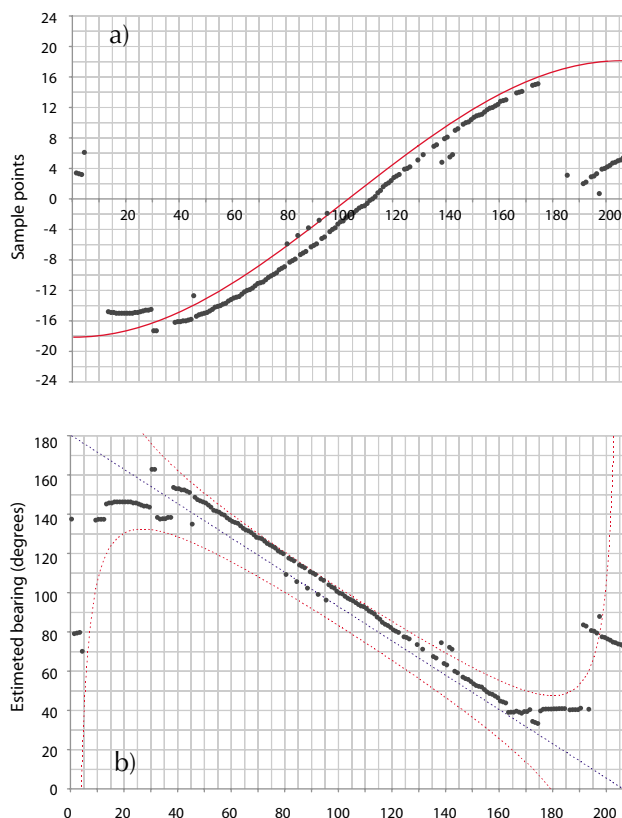


figure 9: $r = 0.8\text{m}$, Anti-clockwise rotation; a) measured phase shift x over the series of measurements; b) estimated bearings with error margin over the series of measure-

in the test pool with $r = 0.8\text{m}$ for clockwise and anti-clockwise rotation. The top graphs show the phase shift x (in sample points) over the series of measurements while the bottom graphs shows the estimated bearings over the series of measurements.

Figure 10 gives another pair of graphs which plots the estimated bearings over the series of measurements showing clockwise and anti-clockwise rotation in the test pool with $r = 2.4\text{m}$.

Figure 11 gives a pair of graphs which plots the estimated bearings over the series of measurements showing clockwise and anti-clockwise rotation in the lake Burley Griffin with $r = 1.5\text{m}$ and $r = 2.2\text{m}$.

In all the test pool experiments, the receiving hull was rotated by 180° while the rotation was only 100° in the lake experiment presented in figure 11. This was due to obstruction by the pier.

The symmetry of the clockwise and anti-clockwise plots displays the repeatability of measurements and also reveals some features of the environment. The breaking off of the almost linear plots at certain points suggests strong reflections off the environ-

ment. In the test pool, the reflections are suspected to be off the pool wall while in the lake figure 11.a shows a strong reflection off the pier while figure 11.b shows soft reflections which are probably due to the underwater plants in close proximity to the pier.

Analysis of Results

The non-linearity of the sending and receiving transducers seem to have a detrimental effect on original MLS signals introducing a high pass filtering with (figure 12) due to the resonance of the AQ2000 hydrophones. As receivers, these hydrophones have a flat frequency response from DC to approximately 10kHz , but as projectors, they are most efficient near its resonance frequency ($f_c \approx 20\text{kHz}$). However, still the cross-correlation of the received signals provides the bearing information with lowered precision. The introduced frequency filtering results in an uncertainty of x (δx) of approximately ± 3 samples. By considering the uncertainties for all quantities involved and substituting (6) in (1); $\delta d = \pm 0.01\text{m}$, $\delta r = \pm 0.01\text{m}$, $\delta v_a = \pm 10\text{ms}^{-1}$, $\delta f_s = \pm 0.0\text{Hz}$ the

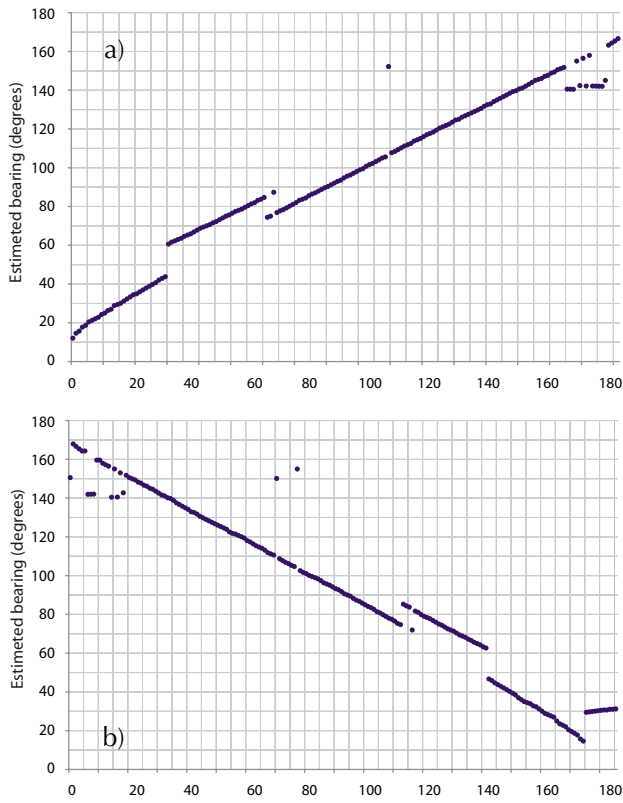


figure 10: Estimated bearings over the series of measurements obtained at the test pool; $r = 2.4$ m, a) Clockwise rotation; b) Anti-clockwise rotation;

following error formula for the estimated bearing is obtained:

$$\delta\theta_e = \pm \sqrt{\frac{6.2^{12} + 6.9 \times 10^9 x^2}{9.2 \times 10^3 - 2.5 \times 10^1 x^2}} \times \left(\frac{3.6 \times 10^{-7}}{\pi}\right)^\circ \quad (7)$$

This translates to a maximum nominal error bound of $\pm 8^\circ$ for $60^\circ \leq \theta_e \leq 120^\circ$. In figure 8.a and 9.a the solid red curve depicts the ideal variation of x as θ is varied. In figure 8.b and 9.b the dashed blue line depicts the ideal variation of θ_e while the two dashed red curves denote the maximum error bound corresponding to $\theta_e \pm \delta\theta_e$.

As it can be observed from these plots, the resulting bearing estimates lie well within the error bounds for most of the measurements. The deviations at the two extremes of can be explained by examining (1); when δ approaches d the uncertainty of θ_e approaches $\pm 180^\circ$. Furthermore the hydrophones used in this experiment are directional with an approximate forward opening angle of 180° within the operating range and frequency. When the arriving signals reach the sensitivity boundary of the receiving hydrophones, the probability of one or both of them detecting a signal bounced off the pool wall instead of the direct signal increases.

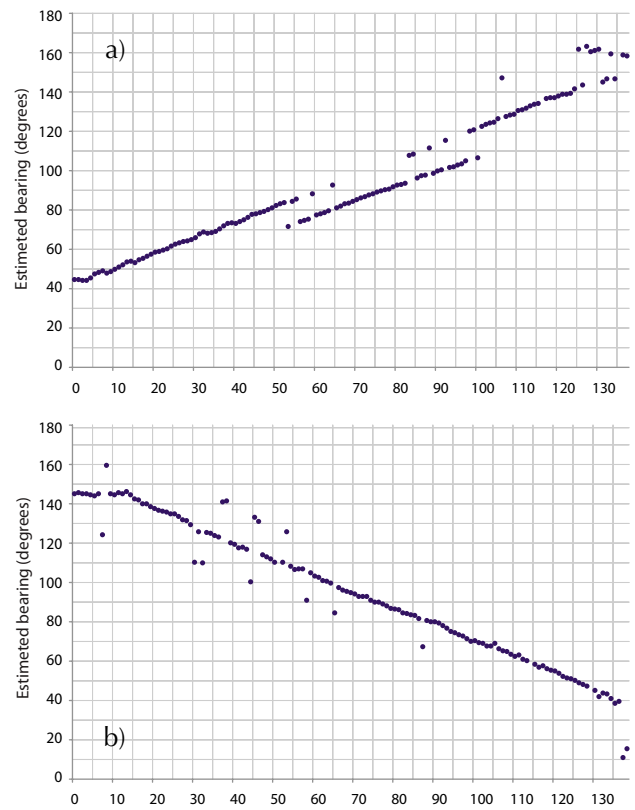


figure 11: Estimated bearings over the series of measurements obtained at the lake; a) Clockwise rotation with $r = 1.5$ m; b) Anti-clockwise rotation with $r = 2.2$ m;

4. Conclusions

From the results of the presented experiments it can be concluded that this approach can be successfully implemented to measure relative bearing and posture of underwater vehicles – even with the frequency filtering introduced by the sending and receiving hydrophones. While it seems obvious that the achieved resolution and precision can be improved by the employment of more wide-band, omni-directional transducers, and higher sampling rates, it is already sufficient for the problem at hand. In all the experiments, it was noted that the bearing estimate plot showed a linear variation with the measurements for at least an opening angle of 100° ($40^\circ \leq \theta_e \leq 140^\circ$). Since more than one pair of receivers would be utilised in the actual implementation on the Serafina vehicle, this result shows just two pairs of receiving hydrophones could cover the full field of 360° around each vehicle on a plane. Three pairs would extend measurements to cover all three dimensions.

Furthermore, in this experimental setup the receiver hydrophones were constantly moving while the measurements were taken in contrast to the stationary hydrophones in the experiments presented in [7].

This suggests the bearing estimation system is not sensitive to motion. The experimental results obtained in the lake suggests that the system is robust enough to perform well in a real underwater environment.

Other experiments and extensions which will be implemented in close future include: Measurement of the ratio of employed energy to achievable minimum error and maximal range with respect to bearing as well as the control of a bounded range for the acoustical based estimations. A bounded range is in fact essential for scaling up to larger schools of vehicles as otherwise multiple measurements in the same school could not take place without interference.

The Serafina project will incorporate the results presented here and integrate these estimates into the existing and further developed control and communication concepts which would be utilised in implementing swarming behavior in schools of submersibles.

References

- [1] Shahab Kalantar, Uwe R. Zimmer; *Control of Open Contour Formations of Autonomous Underwater Vehicles*; International Journal of Advanced Robotic Systems, Dec. 2005
- [2] Shahab Kalantar, Uwe R. Zimmer; *Distributed Shape Control of Homogeneous Swarms of Autonomous Underwater Vehicles*; to appear in Autonomous Robots (journal) 2006
- [3] Felix Schill, Uwe R. Zimmer; *Distributed Dynamical Omnicast Routing*; to appear in Intl. Journal of Complex Systems 2006

- [4] W. Wesley Peterson, E.J. Weldon, Jr.; *Error-Correcting Codes*; MIT Press, second edition, 1972
- [5] K. V. Mackenzie, *Nine-term Equation for Sound Speed in the Oceans*; Journal of the Acoustical Society of America, vol. 70(3), pp. 807-812, September 1981.
- [6] J. G. Proakis, D. G. Manolakis, *Digital Signal Processing: Principles, Algorithms, and Applications*, 3rd ed., New Jersey: Prentice Hall, 1996, pp.130-132.
- [7] Navinda Kottege, Uwe R. Zimmer; *Acoustic Localization in Schools of Submersibles*; Proceedings of the IEEE Oceans 2006, Singapore, May 2006.
- [8] Ethem M. Sozer, Milica Stojanovic, and John G. Proakis, *Underwater acoustic networks*; IEEE Journal of Oceanic Engineering, vol. 25(1), pp. 72-83, January 2000.
- [9] Daniel B. Kilfoyle, Arthur B. Baggeroer; *The State of the Art in Underwater Acoustic Telemetry*; IEEE Journal of Oceanic Engineering, vol. 25(1), pp. 4-27, January 2000.
- [10] <http://serafina.anu.edu.au>

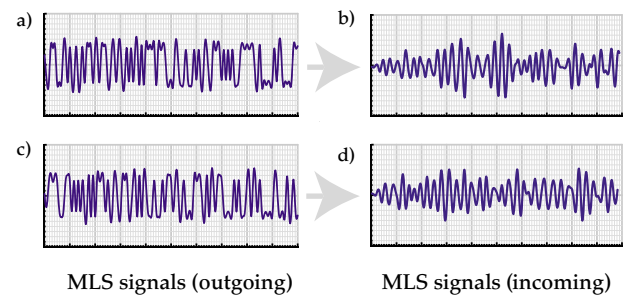


figure 12: Actual MLS signal sent out and the corresponding signals received by the hydrophones